BMC Medical Imaging

RESEARCH

Open Access

Prediction of neoadjuvant chemotherapy efficacy in breast cancer: integrating multimodal imaging and clinical features

Xianglong Chen[1*†], Yong Luo[2†], Zhiming Xie[3†], Yun Wen[2†], Fangsheng Mou[2*] and Wenbing Zeng[2*]

Abstract

Objectives To assess the predictive value of combining DCE-MRI, DKI, IVIM parameters, and clinical characteristics for neoadjuvant chemotherapy (NAC) efficacy in invasive ductal carcinoma.

Methods We conducted a retrospective study of 77 patients with invasive ductal carcinoma, analyzing MRI data collected before NAC. Parameters extracted included DCE-MRI (Ktrans, Kep, Ve, wash-in, wash-out, TTP, iAUC), DKI (MK, MD), and IVIM (D, D*, f). Differences between NAC responders and non-responders were assessed using t-tests or Mann-Whitney U tests. ROC curves and Spearman correlation analyses evaluated predictive accuracy.

Results NAC responders had higher DCE-MRI-Kep, DKI-MD, IVIM-D, and IVIM-f values. Non-responders had higher DCE-MRI-Ve, DKI-MK, IVIM-D (kurtosis, skewness, entropy), and IVIM-f (entropy). The mean DKI-MK had the highest AUC (0.724), and IVIM-D interquartile range showed the highest sensitivity (94.12%). Combined parameters had the highest AUC (0.969), sensitivity (94.12%), and specificity (90.70%). HER2 status (OR, 0.187; 95% CI: 0.038, 0.914; $P=0.038$) and tumor margin (OR, 20.643; 95% CI: 2.892, 147.365; $P=0.003$) were identified as independent factors influencing the lack of significant efficacy of neoadjuvant chemotherapy (NAC) in breast cancer.

Conclusions Combining DCE-MRI, DKI, and IVIM parameters effectively predicts NAC efficacy, providing valuable preoperative assessment insights.

Clinical trial number Not applicable.

Advances in knowledge

This study innovatively integrates DCE-MRI, DKI, and IVIM imaging techniques and utilizes histogram-based analysis to enhance the prediction accuracy of neoadjuvant chemotherapy efficacy. It not only broadens the application

†Xianglong Chen, Yong Luo, Zhiming Xie and Yun Wen are co-first authors.

*Correspondence:
Xianglong Chen
chenxl202211@163.com
Fangsheng Mou
31390481@qq.com
Wenbing Zeng
422817593@qq.com

Full list of author information is available at the end of the article

range of imaging parameters but also supports the development of personalized treatment plans based on comprehensive data.

Keywords Invasive ductal carcinoma, Neoadjuvant chemotherapy, Diffusion kurtosis imaging, Intravoxel incoherent motion imaging, Dynamic contrast-enhanced, Histogram parameters

Introduction

Breast cancer is currently the most common malignant tumor among women, and both its incidence and mortality are still on the rise, posing a significant threat to women's quality of life and health [1]. Among breast cancers, invasive ductal carcinoma (IDC) is the most common histological type, characterized by strong invasiveness, prone to infiltrating the chest wall, skin, or distant metastases, requiring prompt and effective treatment. Neoadjuvant chemotherapy (NAC) is the first-line treatment for locally advanced breast cancer (LABC), widely applied in clinical practice. Effective NAC prior to surgery can reduce the tumor size, downgrade the tumor stage, eliminate or reduce micrometastases, increase the chances of surgery, and improve both disease-free survival and overall survival rates [2]. Predicting the efficacy of NAC not only enhances the precision of breast cancer treatment but also provides more personalized treatment plans and better prognostic evaluations. Comprehensive assessment through imaging, molecular biomarkers, and clinical indicators enables earlier detection of chemotherapy response and resistance, thus improving the overall treatment outcomes and quality of life for patients. Traditional imaging methods include mammography, ultrasound, CT, and MRI; among these, magnetic resonance imaging (MRI) is the most sensitive and advanced imaging technique for breast cancer diagnosis, improving lesion detection, lesion characteristics, and the degree of surrounding soft tissue invasion [3]. Dynamic contrast-enhanced magnetic resonance imaging (DCE-MRI), diffusion-weighted imaging (DWI), diffusional kurtosis imaging (DKI), and intravoxel incoherent motion (IVIM) are functional imaging techniques that enhance the differentiation and diagnostic accuracy of benign and malignant tumors, assisting in clinical decision-making and treatment efficacy evaluation.

DCE-MRI can potentially reflect tumor angiogenesis, blood flow, and vascular permeability, and it can display tumor morphological features with high spatial resolution, such as tumor size, enhancement pattern, tumor necrosis, chest wall involvement, tumor margins, and internal enhancement changes, which help assess the tumor's response to NAC [4]. Diffusional Kurtosis Imaging (DKI) extends the basic model of DWI by considering the non-Gaussian behavior of water molecule diffusion, improving the description of tissue microstructure. DKI captures higher-order statistical features of water molecule diffusion, such as mean diffusivity (MD) and mean kurtosis (MK), providing more information for quantifying tissue heterogeneity. Compared to DWI, DKI offers more detailed and precise diffusion characteristics, especially in evaluating tissue complexity and tumor heterogeneity. In tumor tissue, due to high cellular density and irregular structures, water molecule diffusion is non-Gaussian, and DKI can reveal this, whereas DWI cannot differentiate anisotropy and complex microstructure within tissues. IVIM models decompose the diffusion signal into two components: the diffusion component (D value) related to microscopic tissue diffusion and the perfusion component (D* value) related to tissue microcirculation [5]. Compared to DWI, IVIM not only assesses the diffusion characteristics of water molecules but also separates the perfusion effects, which is valuable for evaluating tumor microcirculation and perfusion. IVIM provides comprehensive information on tumor perfusion, especially in tumors with a high density of blood vessels, which is more informative than DWI [6–8].

With advancements in medical imaging technology, multimodal imaging has become an essential method for predicting breast cancer treatment efficacy. Compared to traditional single-modality imaging, combining DCE-MRI, DKI, and IVIM can comprehensively reflect the tumor's microstructure and biological characteristics from multiple perspectives. Histogram features, by quantifying the gray-level distribution of images, include common features such as 10th percentile, 90th percentile, energy, entropy, interquartile range, kurtosis, max, min, mean, median, range, skewness, uniformity, and variance. These serve as alternative markers of tumor heterogeneity, capable of quantifying the complex and uneven tumor microenvironment [7]. For example, kurtosis and entropy can reflect tumor tissue heterogeneity and irregularity, while the 10th and 90th percentiles provide information on the distribution of different intensities within the tumor region [8]. These imaging features are closely related to the tumor's biological behavior, microcirculation status, and angiogenesis, providing more precise support for clinical treatment decisions. The integration of multimodal imaging parameters, morphological features, and clinical data (such as ER, PR, HER2, and Ki-67) can improve the accuracy of NAC efficacy prediction. Compared to single imaging methods, this approach better reflects individual tumor variations and promotes the development of personalized treatment for breast cancer [9, 10].

Materials and methods

Study population

A retrospective study was conducted to collect data from 152 breast cancer patients who underwent MRI examinations between January 2021 and October 2023 in the Radiology Department PACS system at our hospital. All patients were female, and after screening, 77 patients met the inclusion criteria. Inclusion criteria: (1) Diagnosis of breast cancer confirmed by biopsy (invasive ductal carcinoma); (2) Pre-neoadjuvant chemotherapy (NAC) MRI scans including 3.0T routine MRI, dynamic contrast-enhanced (DCE), diffusion kurtosis imaging (DKI), and intravoxel incoherent motion (IVIM) sequences; (3) Completion of 6–8 cycles of NAC; (4) Surgical treatment after NAC, with pathological Miller-Payne (MP) grading for efficacy assessment. Exclusion criteria: (1) Poor image quality (motion or artifact interference, low signal-to-noise ratio, insufficient resolution, low contrast); (2) Incomplete patient demographic and clinical data, as shown in Fig. 1.

The Miller-Payne Grading System is a standardized system for assessing the pathological response of breast cancer patients to neoadjuvant chemotherapy (NAC) [11]. It evaluates the pathological changes in tumor tissue,

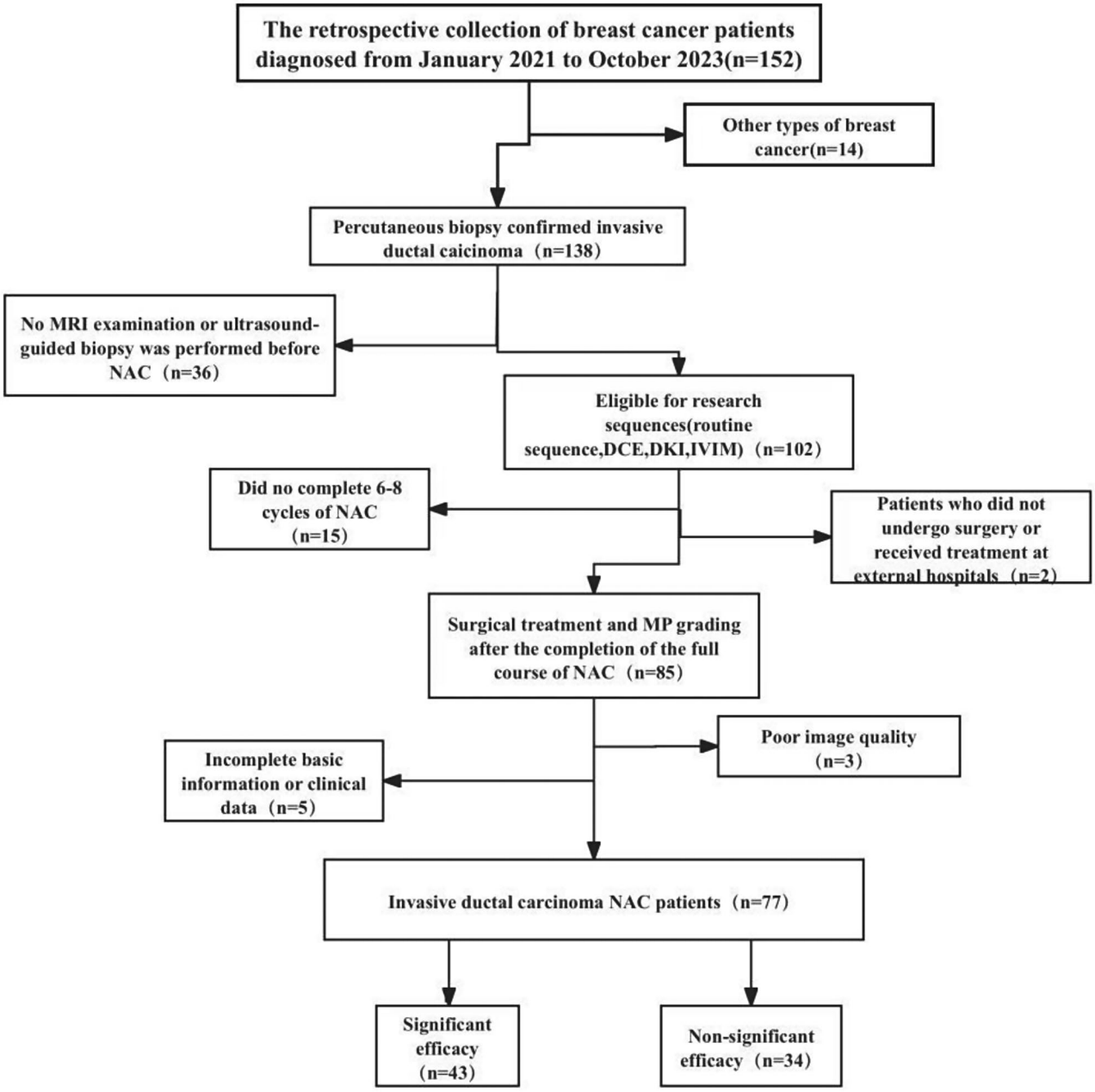

Fig. 1 Flowchart of inclusion and exclusion criteria for breast cancer patients

particularly the changes in tumor cell density. The grading system observes the degree of reduction in tumor cells, especially in terms of tumor necrosis, fibrosis, and changes in cellular density after chemotherapy, providing a precise reflection of NAC efficacy. Patients meeting the inclusion criteria were evaluated for NAC efficacy based on changes in tumor cell density using the Miller-Payne grading system: Grade I: No reduction in tumor cell density; Grade II: Tumor cell density reduced by <30%; Grade III: Tumor cell density reduced by 30-90%; Grade IV: Tumor cell density reduced by >90%, but residual tumor cell clusters or scattered single tumor cells present; Grade V: No residual tumor cells, but ductal carcinoma in situ components may remain [12, 13]. Based on the pathological response of the tumor, imaging results (presence/absence of tumor, abnormal enhancement in the lesion area), and clinical response, Grades IV and V were defined as the significant efficacy group, while Grades I, II, and III were defined as the non-significant efficacy group [14, 15]. The study protocol has been registered with the National Medical Research Registration System and approved by the affiliated medical institution and relevant regulatory departments.

MRI examination protocol

In this study, all cases were scanned using a Siemens 3.0T magnetic resonance imaging (MRI) system with an 18-channel dedicated breast phased-array coil to acquire images. The imaging protocols included axial T1-weighted imaging (T1WI) with a repetition time (TR) of 6.04 ms, echo time (TE) of 2.46 ms, slice thickness of 1.6 mm, field of view (FOV) of 360 mm × 360 mm, acquisition matrix of 448 × 384, and one excitation. For axial T2-weighted imaging (T2WI), the TR was 6500 ms, TE was 84 ms, slice thickness was 4 mm, FOV was 400 mm × 400 mm, acquisition matrix was 448 × 448, with one excitation. Diffusion Kurtosis Imaging (DKI) and Intravoxel Incoherent Motion Imaging (IVIM) used TR of 6100 ms, TE of 54 ms, slice thickness of 4 mm, FOV of 340 mm × 340 mm, and an acquisition matrix of 190 × 190, with b-values set at 50, 450, 800, 1200, and 1600 s/mm². Dynamic Contrast-Enhanced MRI (DCE-MRI) was performed with a TR of 7.14 ms, TE of 3.69 ms, inversion angle of 8°, slice thickness of 4 mm, matrix of 448 × 448, and FOV of 340 mm × 340 mm, with a scan time of 9.6 s per phase for a total of 35 phases. A 20 mL dose of Gadopentetate dimeglumine contrast agent was injected intravenously using a power injector at a rate of 2.0 mL/s, as detailed in Table 1.

Image processing and analysis

The original MR breast DCE, DKI, and IVIM images that met the inclusion criteria were exported from the PACS system in DICOM format and processed using Body Station software for analysis. The DKI model was selected for functional calculation to obtain pseudo-color maps for MD and MK. Manual layer-by-layer delineation of the entire lesion ROI was performed by identifying the lesion on the MRI-enhanced images, ensuring that non-tumor tissue (such as normal tissue, necrosis, liquefaction, large blood vessels) was excluded as much as possible, and then saved. Using the same software, the IVIM model was applied for functional calculation to obtain pseudo-color maps for D, f, and D* values. The DKI lesion ROIs were copied onto the IVIM pseudo-color maps to ensure consistency between the DKI and IVIM lesion delineation.

Additionally, the MR Tissue4D software was used to manually delineate the core lesion area on the enhanced original images, obtaining quantitative parameters for DCE-MRI, including the volume transfer constant (Ktrans), rate constant (Kep), and the extravascular extracellular volume fraction (Ve), as well as semi-quantitative parameters such as wash-in, wash-out, time to peak (TTP), and the initial area under the curve (iAUC) within the first 60 s after contrast injection. This entire process was independently completed by two experienced radiologists under double-blind conditions.

Table 1 MRI scan parameters

Parameters	T1WI	T2Dixon	DKI	IVIM	Twist-Vibe
Spatial resolution, mm	0.8×0.8×1.6	0.9×0.9×4.0	1.8×1.8×4.0	1.8×1.8×4.0	1.0×1.0×4.0
TR/TE, ms	6.04/2.46	6500.00/84.00	6100.00/54.00	5700.00/54.00	7.14/3.69
Slice thickness, mm	1.6	4	4	4	4
Fat saturation	No	Dixon	SPAIR	SPAIR	Water Ex
FOV, mm	360×360	400×400	340×340	340×340	340×340
Temporal resolution, s	53	91	211	211	9.6
Matrix	448×384	448×448	190×190	190×190	448×448
Distance factor, mm	0.32	1	0.8	0.8	4
Bandwidth, Hz/pixel	380	930	1754	1754	590
b value	N/A	N/A	50/450/800/1200/1600	50/450/800/1200/1600	N/A
Flip angles, degree	120	120	120	120	8

Statistical analysis

Statistical analysis was performed using SPSS 25.0 software. The intra-class correlation coefficient (ICC) was used to test the consistency of DCE, DKI, and IVIM histogram parameters between the two groups. The Kolmogorov-Smirnov test was applied to assess whether the continuous variables followed a normal distribution. For variables that followed a normal distribution, data were expressed as mean ± standard deviation ($\bar{x} \pm s$), and intergroup comparisons were performed using the independent two-sample t-test with Bonferroni correction. For variables that did not follow a normal distribution, data were described using median and interquartile range (M (P25, P75)), and comparisons between groups were made using the Mann-Whitney U test. Categorical variables were compared between groups using the chi-squared test or Fisher's exact test, and data were presented as counts (%).Spearman rank correlation analysis was used to assess the correlation between various parameters and the lack of significant NAC efficacy. ROC curves were generated using MedCalc 22.0 software, and the diagnostic performance of each parameter in distinguishing NAC efficacy was evaluated using the area under the curve (AUC). The confidence intervals and odds ratios (OR) were calculated using the bootstrap method. The DeLong method was applied to compare the AUC differences between parameters to determine whether the differences were statistically significant ($P<0.05$). Variables with $P<0.01$ from univariate (categorical and continuous) logistic regression analysis were included in the multivariate logistic regression analysis to identify independent factors influencing NAC efficacy.

Results

Comparison of clinical data and MRI image characteristics

The results of the intra-class correlation coefficient (ICC) consistency test were as follows: DCE (0.821–0.997), DKI MD value (0.873–0.988), MK value (0.917–0.985), IVIM D value (0.830–0.977), f value (0.803–0.911), and D* value (0.902–0.990). All ICC values were greater than 0.7, indicating good consistency between the two sets of data.

According to the Miller-Payne grading system, the NAC efficacy group was divided into two groups: 6 patients in grade I, 11 patients in grade II, and 17 patients in grade III, which were categorized as the non-significant efficacy group (34 patients); 16 patients in grade IV and 27 patients in grade V, which were categorized as the significant efficacy group (43 patients). There were no statistically significant differences between the significant and non-significant efficacy groups regarding age, menstrual status, lesion quadrant, tumor size, enhancement pattern, peritumoral edema, tumor necrosis, chest wall involvement, skin thickening, nipple retraction, P53 status, immunohistochemical subtype, and axillary lymph node metastasis ($P>0.05$).In this study, for the significant efficacy group, 35 patients (81%) had regular tumor margins, and 8 patients (19%) had star-like margins; in the non-significant efficacy group, 15 patients (44%) had regular margins, and 19 patients (56%) had star-like margins. In the significant efficacy group, 32 patients (74%) had heterogeneous internal enhancement, and 11 patients (26%) had ring-like or segmental enhancement; in the non-significant efficacy group, 17 patients (50%) had heterogeneous internal enhancement, and 17 patients (50%) had ring-like or segmental enhancement.In the significant efficacy group, 32 patients (74%) had low ER expression (≤10%) and 11 patients (26%) had moderate/high ER expression (>10%); in the non-significant efficacy group, 14 patients (41%) had low ER expression and 20 patients (59%) had moderate/high ER expression. In the significant efficacy group, 37 patients (86%) had low PR expression (≤10%) and 6 patients (14%) had moderate/high PR expression (>10%); in the non-significant efficacy group, 18 patients (53%) had low PR expression and 16 patients (47%) had moderate/high PR expression.In the significant efficacy group, 1 patient (2%) had low Ki67 expression (≤14%) and 42 patients (98%) had moderate/high Ki67 expression (>14%); in the non-significant efficacy group, 27 patients (79%) had low Ki67 expression and 7 patients (21%) had moderate/high Ki67 expression.In the significant efficacy group, 14 patients (33%) were HER2-negative and 29 patients (67%) were HER2-positive; in the non-significant efficacy group, 23 patients (68%) were HER2-negative and 11 patients (32%) were HER2-positive. All of these findings were statistically significant ($P<0.05$). Detailed clinical data and MR imaging features of patients with invasive ductal carcinoma of the breast before NAC treatment are shown in Table 2; Fig. 2.

Analysis of DCE, DKI, and IVIM parameters

In the significant efficacy group of breast cancer patients, the DCE-MRI-Kep, DKI-MD (90th Percentile, Mean, Median, Max, Range), IVIM-D (90th Percentile, Interquartile Range, Mean, Median, Variance, Uniformity), and IVIM-f (Interquartile Range) were higher than in the non-significant efficacy group. Meanwhile, the DCE-MRI-Ve, DKI-MK (Mean, Median), IVIM-D (Kurtosis, Skewness, Entropy), and IVIM-f (Entropy) were lower in the significant efficacy group compared to the non-significant efficacy group. All differences between the two groups were statistically significant ($P<0.05$).

In the univariate logistic regression analysis (for both categorical and continuous variables), tumor margin, internal enhancement, ER expression, PR expression, HER2 status, Ki67 expression, DKI-D (90th Percentile, Max, Mean, Median, Range), DKI-K (Mean, Median), IVIM-D (90th Percentile, Entropy, Interquartile Range, Mean, Median, Kurtosis, Skewness, Uniformity,

Table 2 Clinical data and MR imaging features of breast Cancer NAC significant efficacy group and Non-significant efficacy group

	Significant efficacy group (*N* = 43)	Non-significant efficacy group (*N* = 34)	Test statistic	*P* value
Lesion margin			11.59	0.001
Regular	35 (81%)	15 (44%)		
Stellate	8 (19%)	19 (56%)		
Internal enhancement			4.89	0.027
Heterogeneous	32 (74%)	17 (50%)		
Rim enhancement or septations	11 (26%)	17 (50%)		
ER expression			8.72	0.003
Low expression (≤10%)	32 (74%)	14 (41%)		
Intermediate to high expression (>10%)	11 (26%)	20 (59%)		
PR expression			10.2	0.001
Low expression (≤10%)	37 (86%)	18 (53%)		
Intermediate to high expression (>10%)	6 (14%)	16 (47%)		
HER2 status			9.37	0.002
Negative	14 (33%)	23 (68%)		
Positive	29 (67%)	11 (32%)		
Ki67 expression			4.98	0.026
Low expression (≤14%)	1 (2%)	27 (79%)		
Intermediate to high expression (>14%)	42 (98%)	7 (21%)		

Note: Normally distributed data is represented as X± S; non-normally distributed data is represented as M (P25, P75); and count data is represented as frequency (percentage)

Variance), and IVIM-f (Entropy, Interquartile Range) were all significantly associated with NAC efficacy ($P < 0.05$).To enhance the significance and stability of the model, avoid multicollinearity, reduce redundant variables, and control for potential confounding factors, we included variables with $P < 0.01$ in the multivariate binary logistic regression analysis. The results revealed that HER2 status (OR, 0.187; 95% CI: 0.038, 0.914; $P = 0.038$) and tumor margin (OR, 20.643; 95% CI: 2.892, 147.365; $P = 0.003$) were independent factors significantly associated with non-significant NAC efficacy in breast cancer ($P < 0.05$), as detailed in Tables 3, 4 and 5; Figs. 3 and 4.

Correlation analysis of DCE, DKI, and IVIM parameters with NAC efficacy

The results indicated that DCE-MRI-Kep, DKI-MD (90th Percentile, Mean, Median, Max, Range), IVIM-D (90th Percentile, Interquartile Range, Mean, Median, Variance, Uniformity), and IVIM-f (Interquartile Range) were positively correlated with the significant efficacy of neoadjuvant chemotherapy (NAC) in breast cancer ($r\_s > 0$, $P < 0.05$). This suggests that the larger these parameters, the higher the NAC efficacy. Conversely, DCE-MRI-Ve, DKI-MK (Mean, Median), IVIM-D (Kurtosis, Skewness, Entropy), and IVIM-f (Entropy) were negatively correlated with NAC efficacy ($rs < 0$, $P < 0.05$), indicating that the larger these parameters, the lower the NAC efficacy.

Among these parameters, DCE-MRI-Ve had the highest correlation with NAC efficacy ($rs = 0.267$). For DKI-MD, the Max and Range values exhibited the highest correlation with NAC efficacy ($rs = 0.357$). In DKI-MK, the Mean value showed the highest correlation with NAC efficacy ($rs = 0.386$). Regarding IVIM-D, the Mean value had the highest correlation with NAC efficacy ($rs = 0.367$), and for IVIM-f, the Interquartile Range demonstrated the highest correlation with NAC efficacy ($rs = 0.296$), as detailed in Table 6.

Diagnostic efficacy analysis of individual and combined Whole-Histogram parameters

Among the single parameters, the DKI-MK Mean value had the largest area under the ROC curve (AUC = 0.724), while the IVIM-D Interquartile Range exhibited the highest sensitivity (94.12%). The DKI-MK Mean and IVIM-D Median values showed the highest specificity (90.70%). In terms of combined parameters, the AUC, sensitivity, and specificity were highest when DCE-MRI was combined with DKI and IVIM histogram parameters, with values of 0.969, 94.12%, and 90.70%, respectively.There were no significant differences in AUC between the single parameters ($P > 0.05$). However, significant differences in AUC were observed between the combined DCE parameter and the combinations of IVIM, DKI + IVIM, and DCE + DKI + IVIM ($P < 0.05$). Additionally, significant differences were found between the combined DKI parameter and the DKI + IVIM and DCE + DKI + IVIM combinations ($P < 0.05$). Similarly, significant differences were seen between the IVIM parameter and the DKI + IVIM and DCE + DKI + IVIM combinations ($P < 0.05$), as detailed in Table 6; Fig. 5.

Discussion

Predictive value of pre-NAC MRI imaging characteristics, clinical features, and immunohistochemical factors for NAC efficacy in invasive ductal carcinoma of the breast

In this study, the preoperative lesion margin, internal enhancement patterns, ER expression, PR expression, Ki67 expression, and Her2 status in breast cancer patients were all statistically significantly associated with the efficacy of NAC. The number of patients with significant therapeutic effects and a star-shaped lesion margin was significantly lower compared to those with a regular lesion margin, which may be attributed to the high activity and rapid proliferation rate of tumor cells, resulting in a high cell density and infiltration into surrounding

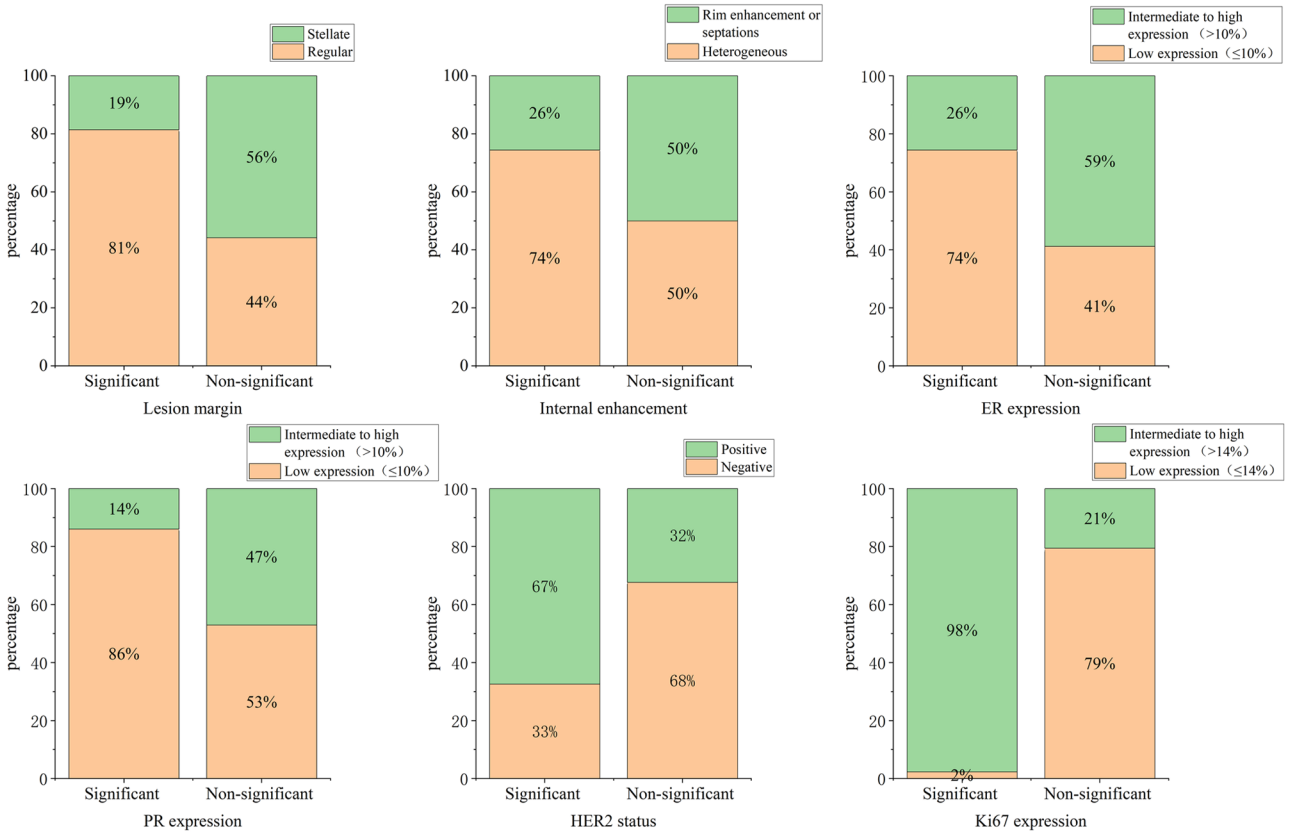

Fig. 2 Comparison of categorical variables between the significant efficacy group and the non-significant efficacy group ($P < 0.05$)

Table 3 Comparison of global histogram parameters in breast cancer NAC (Significant efficacy group vs. Non-significant efficacy group)

Variable	Significant efficacy group ($N = 43$)	Non-significant efficacy group ($N = 34$)	t/Z value *P* value	*P* value
DCE-Kep	0.646 (0.526, 0.806)	0.556 (0.456, 0.645)	-1.980	0.048
DCE-Ve	0.077 (0.057, 0.126)	0.105 (0.082, 0.163)	-2.329	0.020
DKI-MD-90Percentile	2.355 ± 0.396	2.100 ± 0.424	2.721	0.008
DKI-MD-Max	3.559 (2.890, 4.250)	2.684 (2.249, 3.690)	-3.108	0.002
DKI-MD-Mean	1.582 (1.421, 1.710)	1.459 (1.254, 1.652)	-2.472	0.013
DKI-MD-Median	1.610 ± 0.305	1.419 ± 0.279	2.838	0.006
DKI-MD-Range	3.550 (2.852, 3.988)	2.741 (2.261, 3.256)	-3.108	0.002
DKI-MK-Mean	0.871 (0.777, 0.992)	1.054 (0.899, 1.266)	-3.365	0.001
DKI-MK-Median	0.869 (0.772, 0.934)	0.986 (0.813, 1.155)	-2.934	0.003
IVIM-D-90Percentile	1.373 ± 0.295	1.205 ± 0.213	2.801	0.006
IVIM-D-Entropy	0.532 (0.484, 0.552)	0.538 (0.518, 0.575)	-2.088	0.037
IVIM-D-InterquartileRange	0.435 ± 0.152	0.331 ± 0.120	3.275	0.002
IVIM-D-Kurtosis	0.302 (0.274, 0.350)	0.347 (0.286, 0.409)	-2.175	0.030
IVIM-D-Mean	0.953 ± 0.203	0.836 ± 0.139	2.876	0.005
IVIM-D-Median	0.932 (0.865, 0.987)	0.882 (0.745, 0.947)	-2.729	0.006
IVIM-D-Skewness	0.102 ± 0.486	0.409 ± 0.685	-2.210	0.031
IVIM-D-Uniformity	0.375 (0.325, 0.428)	0.289 (0.219, 0.350)	-2.232	0.026
IVIM-D-Variance	1.199 ± 0.604	0.875 ± 0.490	2.542	0.013
IVIM-f-Entropy	0.356 ± 0.041	0.376 ± 0.033	-2.304	0.024
IVIM-f-InterquartileRange	0.158 (0.128, 0.191)	0.120 (0.091, 0.172)	-2.580	0.010

Note: Normally distributed data is represented as X ± S; non-normally distributed data is represented as M (P25, P75); and count data is represented as frequency (percentage)

Table 4 Univariate binary logistic regressioen analysis of neoadjuvant chemotherapy (NAC) efficacy in invasive ductal carcinoma of the breast

	Coefficient	Standard error	Wald	Degrees of freedom	Significance	OR	95% confidence interval for OR	
							Lower limit	Upper limit
Lesion margin	1.712	0.522	10.745	1	0.001	5.542	1.991	15.427
Internal enhancement	1.068	0.490	4.755	1	0.029	2.909	1.114	7.596
ER expression	1.425	0.494	8.331	1	0.004	4.156	1.580	10.934
PR expression	1.701	0.558	9.285	1	0.002	5.481	1.835	16.374
HER2 status	-1.604	0.498	10.388	1	0.001	0.201	0.076	0.533
Ki67 expression	-2.388	1.097	4.736	1	0.030	0.092	0.011	0.789
DCE-Kep	-1.084	0.852	1.618	1	0.203	0.338	0.064	1.798
DCE-Ve	2.819	1.793	2.471	1	0.116	16.755	0.499	562.846
DKI-D-90Percentile	-0.002	0.001	6.305	1	0.012	0.998	0.997	1.000
DKI-D-Max	-0.001	0.000	5.496	1	0.019	0.999	0.999	1.000
DKI-D-Mean	-0.003	0.001	6.834	1	0.009	0.997	0.995	0.999
DKI-D-Median	-0.002	0.001	6.683	1	0.010	0.998	0.996	0.999
DKI-D-Range	-0.001	0.000	5.133	1	0.023	0.999	0.999	1.000
DKI-K-Mean	0.004	0.001	10.220	1	0.001	1.004	1.002	1.007
DKI-K-Median	0.004	0.002	8.345	1	0.004	1.004	1.001	1.007
IVIM-D-90Percentile	-0.003	0.001	6.621	1	0.010	0.997	0.996	0.999
IVIM-D-Entropy	1.216	0.546	4.966	1	0.026	3.373	1.158	9.825
IVIM-D-InterquartileRange	-0.006	0.002	8.525	1	0.004	0.994	0.991	0.998
IVIM-D-Kurtosis	0.642	0.323	3.942	1	0.047	1.900	1.008	3.581
IVIM-D-Mean	-0.004	0.001	6.820	1	0.009	0.996	0.993	0.999
IVIM-D-Median	-0.005	0.002	6.603	1	0.010	0.995	0.991	0.999
IVIM-D-Skewness	0.920	0.423	4.737	1	0.030	2.510	1.096	5.747
IVIM-D-Uniformity	-38.850	19.255	4.071	1	0.044	0.000	0.000	0.329
IVIM-D-Variance	0.000	0.000	5.587	1	0.018	1.000	1.000	1.000
IVIM-f-Entropy	1.524	0.705	4.682	1	0.030	4.593	1.154	18.27
IVIM-f-InterquartileRange	-0.009	0.004	4.067	1	0.044	0.991	0.983	1.000

Table 5 Multivariable binary logistic regression analysis of neoadjuvant chemotherapy (NAC) efficacy in invasive ductal carcinoma of the breast

	Coefficient	Standard error	Wald	Degrees of freedom	Significance	OR	95% confidence interval for OR	
							Lower limit	Upper limit
DKI-D-Mean	-0.002	0.002	2.32	1	0.128	0.998	0.995	1.001
DKI-K-Mean	0.003	0.005	0.261	1	0.609	1.003	0.992	1.013
DKI-K-Median	0.003	0.006	0.201	1	0.654	1.003	0.992	1.014
IVIM-D-InterquartileRange	-0.003	0.003	1.171	1	0.279	0.997	0.991	1.003
IVIM-D-Mean	-0.004	0.002	2.719	1	0.099	0.996	0.992	1.001
Lesion margin	3.027	1.003	9.113	1	0.003	20.643	2.892	147.365
ER expression	0.733	1.191	0.379	1	0.538	2.081	0.201	21.503
PR expression	0.749	1.317	0.323	1	0.570	2.115	0.16	27.956
HER2 status	-1.674	0.808	4.29	1	0.038	0.187	0.038	0.914

tissues, leading to fibrosis and a star-shaped margin appearance [16, 17]. This may cause the NAC effect to be less significant. In contrast, the number of patients with significant therapeutic effects and uneven internal enhancement was significantly higher compared to those with ring or segmented enhancement. This may be due to insufficient angiogenesis, the presence of necrotic or fibrotic areas within the tumor, which usually have poor blood and oxygen supply, making it difficult for therapeutic agents to penetrate effectively, thus limiting the treatment efficacy [18].

According to the latest guidelines from the American Society of Clinical Oncology (ASCO) and the College of American Pathologists (CAP), ER and PR immunohistochemical (IHC) staining levels of 1–10% are classified as low expression. In this study, the number of patients

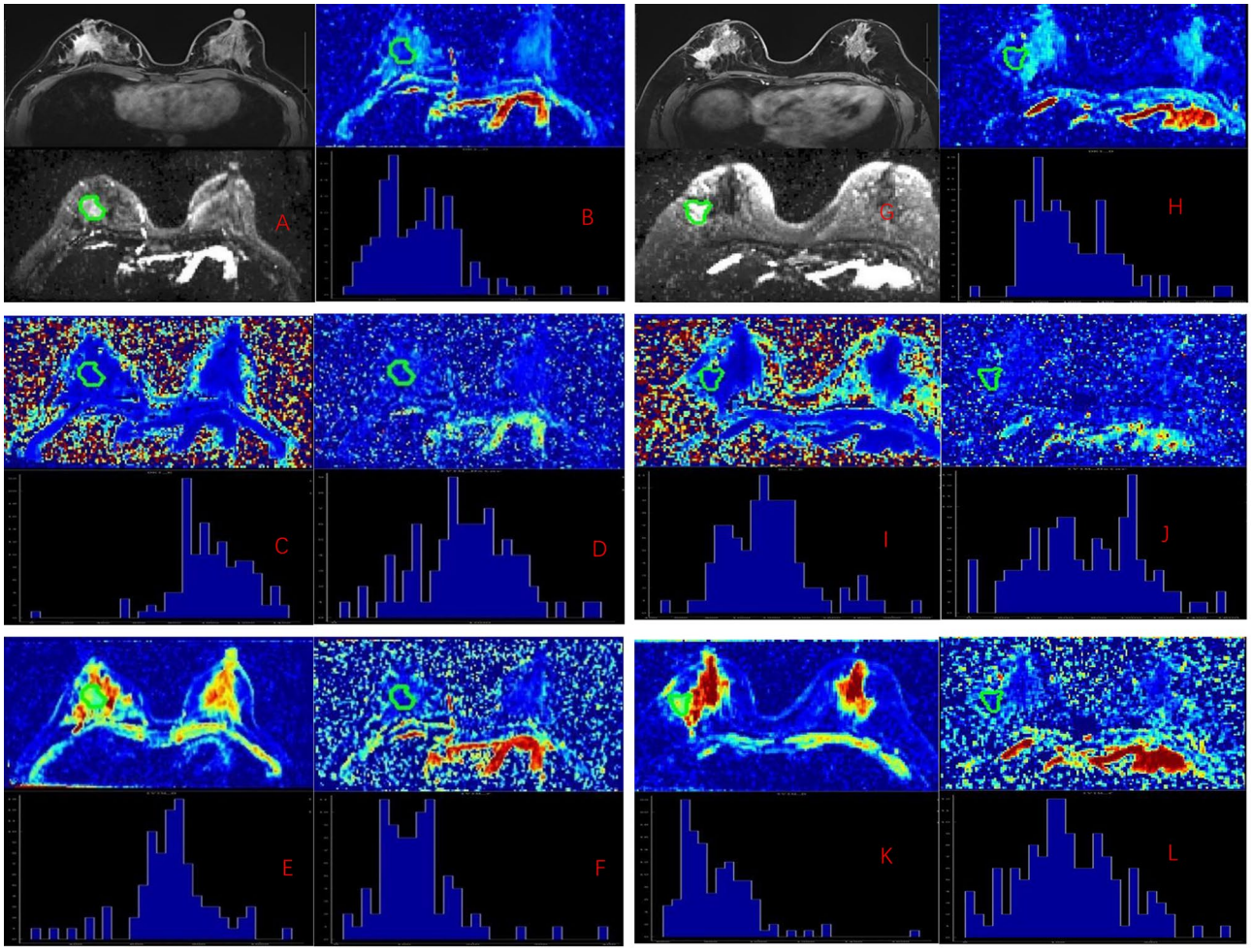

Fig. 3 **A**∼**F** represents patients in the non-significant neoadjuvant chemotherapy (NAC) group, with tumor lesions in the upper outer quadrant of the breast. Pathological results indicate invasive ductal carcinoma with heterogeneous enhancement. Regions of interest (ROI) were delineated globally on the DKI raw images (**A**), then copied onto the color maps of MD (**B**), MK (**C**), D* value (**D**), D value (**E**), and f value (**F**), with global histogram parameters calculated. **G**∼**L** represents patients in the significant neoadjuvant chemotherapy (NAC) group, with tumor lesions in the right upper outer quadrant of the breast. Pathological results indicate invasive ductal carcinoma with heterogeneous enhancement. Regions of interest (ROI) were delineated globally on the DKI raw images (**G**), then copied onto the color maps of MD (**H**), MK (**I**), D* value (**J**), D value (**K**), and f value (**L**), with global histogram parameters calculated

with low ER and PR expression and significant NAC efficacy was significantly higher than that of patients with medium/high expression. Low ER and PR expression in breast cancer may indicate that the tumor is less dependent on estrogen and progesterone for growth, which may result in higher resistance to hormone therapy [19]. Therefore, these patients may respond better to NAC, which works through a different mechanism.

The expression levels of human epidermal growth factor receptor 2 (Her2) are classified into four grades, from 0 to 3+, with IHC results of 3 + or 2 + combined with in situ hybridization (ISH) showing positivity being considered Her2-positive. In this study, the number of Her2-positive patients with significant NAC efficacy was significantly higher than that of Her2-negative patients. Her2 is a cell membrane receptor that plays an important role in regulating cell growth and division. Her2-positive breast cancer cells usually have higher proliferative activity, and these tumor cells may be more sensitive to chemotherapy drugs [20, 21].

In previous studies, Ki67 IHC staining levels of 1–14% were considered low expression [22]. In this study, the number of patients with significant NAC efficacy and low Ki67 expression was significantly lower than that of patients with medium/high expression. Ki67 medium/high expression reflects a higher proliferative activity of tumor cells. During NAC, chemotherapy drugs mainly target rapidly proliferating cancer cells, and therefore, tumors with medium/high Ki67 expression are more likely to be killed by chemotherapy drugs [23, 24].

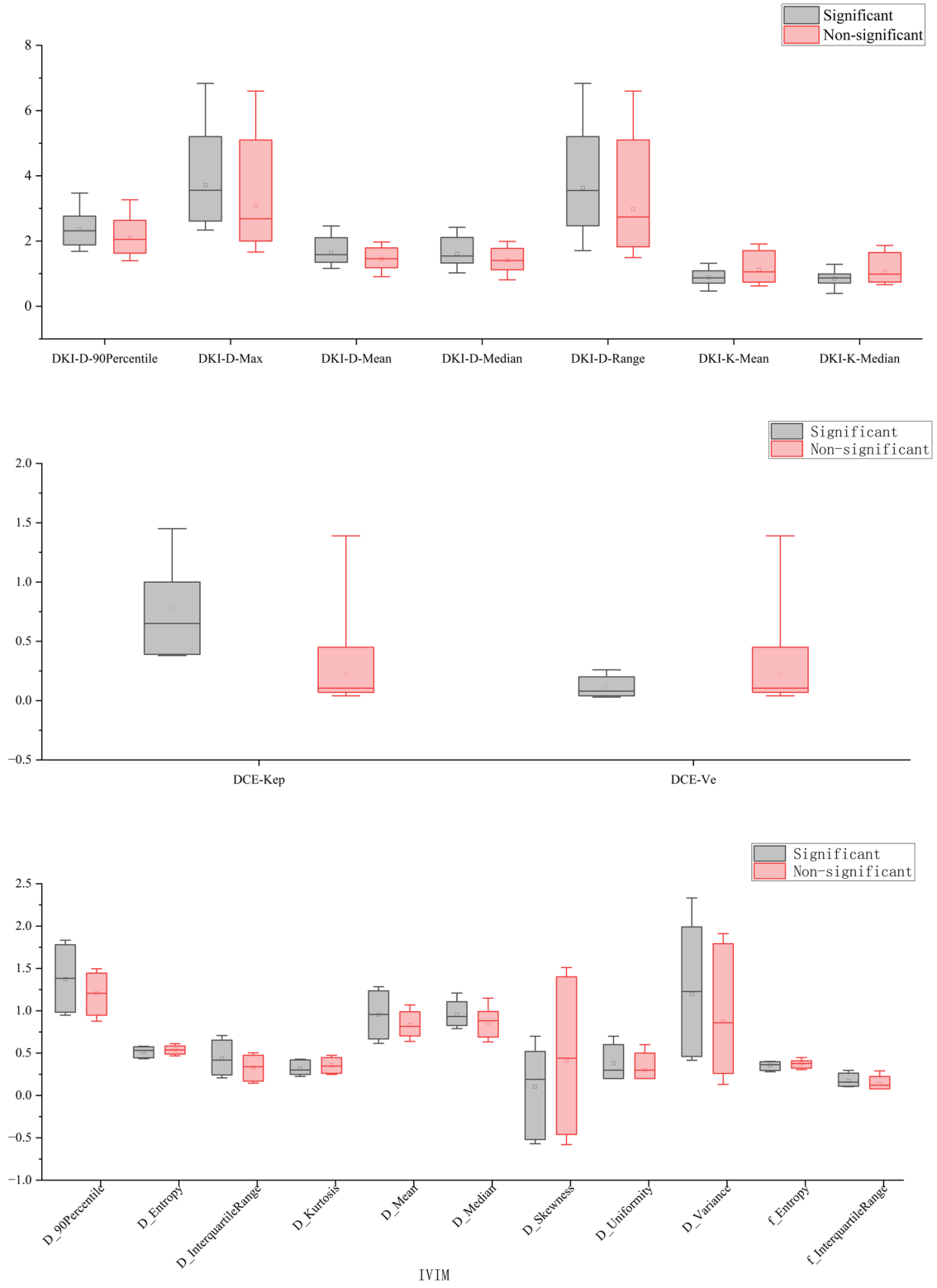

Fig. 4 Comparison of whole-lesion histogram parameters between significant efficacy group and non-significant efficacy group ($P < 0.05$)

Table 6 Analysis of the correlation and diagnostic performance between quantitative and semi-quantitative parameters of DCE-MRI, as well as global histogram parameters of DKI and IVIM, and the non-significant efficacy of neoadjuvant chemotherapy (NAC) in breast cancer

	Correlation coefficient (rs)[a]	AUC	95%CI	Sensitivity (%)	Specificity (%)	PPV	NPV	Accuracy
DCE-Kep	-0.227	0.632	0.515–0.739	76.47	51.16	0.553	0.733	0.623
DCE-Ve	0.267	0.647	0.530–0.753	85.29	44.19	0.547	0.791	0.623
DKI-D-90Percentile	-0.299	0.674	0.557–0.776	50.00	81.40	0.680	0.673	0.675
DKI-D-Max	-0.357	0.707	0.593–0.805	67.65	72.09	0.657	0.738	0.701
DKI-D-Mean	-0.284	0.665	0.548–0.768	41.18	90.7	0.778	0.661	0.688
DKI-D-Median	-0.290	0.669	0.552–0.772	50.00	83.72	0.708	0.679	0.688
DKI-D-Range	-0.357	0.707	0.593–0.805	73.53	69.77	0.657	0.769	0.714
DKI-K-Mean	0.386	0.724	0.611–0.820	70.59	67.44	0.631	0.743	0.688
DKI-K-Median	0.337	0.696	0.580–0.795	58.82	81.40	0.714	0.714	0.714
IVIM-D-90Percentile	-0.317	0.684	0.568–0.785	88.24	46.51	0.566	0.833	0.649
IVIM-D-Entropy	0.239	0.639	0.522–0.746	47.06	79.07	0.640	0.653	0.649
IVIM-D-InterquartileRange	-0.339	0.697	0.582–0.797	94.12	41.86	0.561	0.900	0.649
IVIM-D-Kurtosis	0.250	0.645	0.528–0.751	58.82	67.44	0.588	0.674	0.636
IVIM-D-Mean	-0.367	0.713	0.559–0.811	64.71	79.07	0.709	0.739	0.727
IVIM-D-Median	-0.313	0.682	0.556–0.783	44.12	90.70	0.789	0.672	0.701
IVIM-D-Skewness	0.224	0.630	0.513–0.738	55.88	76.74	0.655	0.687	0.675
IVIM-D-Uniformity	-0.256	0.642	0.525–0.748	41.18	81.40	0.636	0.636	0.636
IVIM-D-Variance	-0.287	0.667	0.550–0.770	85.29	51.16	0.579	0.814	0.662
IVIM-f-Entropy	0.247	0.644	0.526–0.750	79.41	46.51	0.539	0.740	0.610
IVIM-f-InterquartileRange	-0.296	0.672	0.556–0.775	52.94	81.40	0.692	0.686	0.688
DCE		0.676	0.560–0.778	91.18	37.21	0.534	0.842	0.610
DKI		0.826	0.722–0.903	70.59	90.70	0.857	0.795	0.818
IVIM		0.885	0.792–0.947	100.00	62.79	0.679	1.000	0.792
DKI + IVIM		0.950	0.875–0.987	91.18	88.37	0.861	0.926	0.896
DCE + DKI + IVIM		0.969	0.901–0.995	94.12	90.70	0.888	0.951	0.922

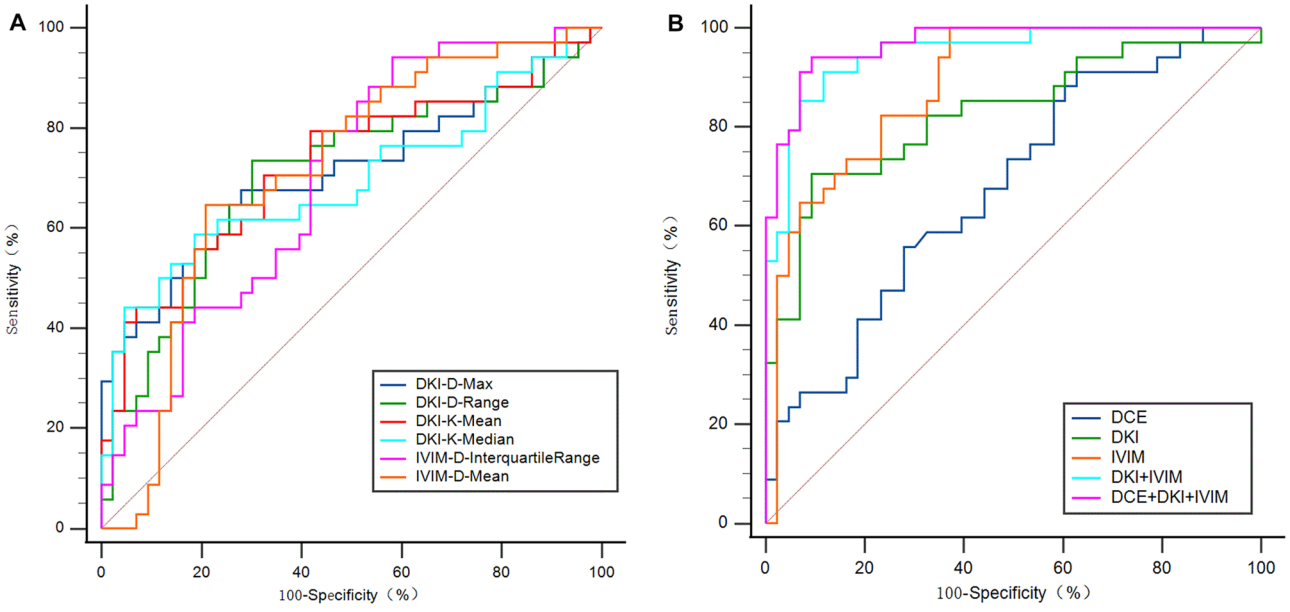

Fig. 5 The ROC curve for independent histogram parameters with higher diagnostic efficacy (**A**) and the ROC curve for combined histogram parameters (**B**)

Value of pre-treatment quantitative parameters (Ktrans, Kep, Ve) and semi-quantitative parameters (Wash-in, Wash-out, TTP, and iAUC) in predicting NAC efficacy in invasive ductal carcinoma of the breast

DCE-MRI quantitative and semi-quantitative parameters can accurately reflect tumor neovascular density, blood flow, and vessel wall permeability. In this study, the pre-treatment quantification of Kep and Ve parameters showed a statistically significant correlation with NAC efficacy. The results indicated that the average Kep value in the NAC-effective group was higher than that in the non-effective group, while the average Ve value was lower in the effective group compared to the non-effective group. Kep reflects the exchange rate between the extracellular space (EES) and blood vessels, while Ve indicates the size of the extracellular space, both of which are related to vascular permeability. As Kep and Ve values increase, the drug is more likely to penetrate and reach the lesion, enhancing the NAC efficacy.

However, the results of this study revealed that the Ve value in the effective group was lower than that in the non-effective group. Although Ve reflects the proportion of extracellular fluid in the tumor, it does not have a direct correlation with chemotherapy effects like tumor cell death, necrosis, or apoptosis, particularly in the early stages of chemotherapy. The tumor microenvironment changes might not immediately affect the Ve value.

Previous studies have shown that longitudinal changes in Kep values, particularly after the second cycle of NAC, could predict overall treatment efficacy. In those studies, the Kep value significantly decreased two weeks after treatment in the PCR group, while the Ve value showed no significant change [25, 26]. Importantly, predicting NAC efficacy before treatment is more desirable in clinical settings. Single baseline parameter predictions of NAC efficacy can have considerable errors, emphasizing the necessity of combining multi-parametric MRI techniques to predict NAC efficacy before treatment.

Value of histogram parameters MD and MK from the DKI model in predicting NAC efficacy in invasive ductal carcinoma of the breast

In the DKI model, the parameter MD reflects the overall diffusion level of water molecules and the resistance to diffusion, while MK mainly indicates the complexity of tissue microstructure [27]. In this study, the results showed that the NAC-effective group had higher MD values (90th Percentile, mean, median, max, and range) compared to the non-effective group. The 90th Percentile value may represent regions within the lesion with lower cellular density, such as necrotic, liquefied, or cystic areas. Higher mean and median values suggest lower cellular density within the lesion, with expanded tissue gaps, allowing for increased diffusion of water molecules and decreased resistance, thus enhancing water content in the tissue [28]. Higher max and range values may indicate that the areas with the most free diffusion of water molecules and lower cellular density are more abundant within the lesion.

On the other hand, the MK values (mean, median) in the NAC-effective group were lower than those in the non-effective group. These values may be associated with tumor cell heterogeneity and microstructural complexity [29]. Lower mean and median values suggest a lower degree of deviation in the distribution of water molecule diffusion displacement and a less complex structure. The results indicate that in the NAC-effective group, MD values (90th Percentile, mean, median, max, range) were higher, while MK values (mean, median) were lower than in the non-effective group. This suggests that before NAC, tumors in the effective group had lower cellular density, less heterogeneity, and less complex microstructures, which is indicative of a better response to NAC. These findings are consistent with baseline study results by Zheng et al. [30].

Predictive value of histogram parameters D, F, and D from the IVIM model in pre-treatment assessment of NAC efficacy for invasive ductal carcinoma of the breast

In the IVIM model, the parameters D and f reflect the true diffusion coefficient of water molecules and perfusion information, respectively [31]. The results of this study showed that in the NAC-effective group, the values of IVIM-D (90th Percentile, Interquartile Range, Mean, Median, Variance, Uniformity) and IVIM-f (Interquartile Range) were higher than those in the non-effective group. Higher IVIM-D (Mean, Median, Variance) values may be associated with lower tumor cell density, larger extracellular spaces, and lower diffusion resistance for water molecules. These areas with reduced diffusion resistance align with the DKI-MD results, where lower resistance facilitates greater diffusion. Additionally, higher values of IVIM-D and IVIM-f (Interquartile Range) may indicate a wider distribution of water molecule diffusion or perfusion values within the tissue, suggesting effective drug penetration during NAC.

On the other hand, the IVIM-D (Kurtosis, Skewness, Entropy) and IVIM-f (Entropy) values were lower in the NAC-effective group, which may reflect higher tissue heterogeneity, uneven water molecule diffusion, and greater dispersion. This indicates less significant NAC efficacy, a result consistent with Kim et al.'s study [32]. In this study, no significant difference in IVIM-D* values was found between the two groups. This suggests that IVIM-D* may have a lower sensitivity to tumor blood perfusion characteristics, as it primarily reflects the perfusion effects of microvessels, while NAC not only affects blood flow but also includes mechanisms such as cell proliferation,

apoptosis, and necrosis. Therefore, D* values may not comprehensively reflect the complex effects of chemotherapy on tumors, especially when tumor microenvironment changes occur. The change in D* values may not be as sensitive or consistent as other imaging parameters (such as Ktrans, MD, etc.) [33].

Baseline studies predict NAC efficacy in invasive ductal carcinoma of the breast without observing dynamic changes of variables during NAC. However, the integration of multi-parametric imaging and clinical features provides a more comprehensive reflection of the correlation between breast cancer lesions and NAC efficacy, offering an effective reference for clinical treatment planning before NAC.

Clinical application and challenges of multimodal imaging and predictive models in predicting neoadjuvant chemotherapy efficacy in breast cancer

In clinical practice, predictive models can be integrated into decision support systems (DSS) to assist oncologists in comprehensively assessing patients based on imaging and clinical features, thereby optimizing neoadjuvant chemotherapy (NAC) treatment plans. Automated image analysis and data integration can rapidly compute tumor-related parameters, provide early efficacy predictions, support the selection of the most appropriate treatment regimen, and allow for regular strategy adjustments based on patient response and imaging changes.

To address the challenges in model application, the first step is to standardize imaging acquisition protocols and ensure data quality consistency through multi-center collaboration and equipment calibration. Additionally, deep learning technologies can be employed to mitigate the impact of equipment variability. Secondly, regular training sessions should be conducted to enhance clinicians' understanding and operational skills in multimodal imaging analysis and predictive modeling, boosting their confidence and competency. Furthermore, large-scale multi-center studies are necessary to validate the stability and reliability of the models and optimize their predictive accuracy. Finally, it is essential to encourage clinicians to combine their clinical experience with model outputs for joint decision-making, avoiding excessive reliance on algorithms and ensuring that treatment plans remain personalized and precise. Integrating these predictive models into clinical workflows is expected to improve the accuracy of NAC efficacy predictions in breast cancer, advancing precision medicine, particularly in the realms of personalized treatment and early efficacy assessment.

Limitations of this study

First, this study is based on a single-center dataset with a limited sample size, which may affect the generalizability of the model. A smaller sample size may result in insufficient statistical power, making it challenging to reliably detect the significance of some variables. Second, the study is retrospective in design, which may introduce selection bias, and the quality of the data could be constrained. Prospective studies or multi-center data validation could enhance the reliability of the results. Third, the model was trained and tested solely on internal datasets, which may lead to overfitting and reduce its applicability to independent datasets. External independent cohorts are required for validation to improve the model's robustness. Fourth, the different molecular subtypes of breast cancer (such as Luminal A, Luminal B, triple-negative, and HER2-positive) and variations in chemotherapy regimens result in varying NAC sensitivity. This study did not perform an in-depth analysis of these subtypes and treatment regimens, which could impact the clinical applicability of the model. Fifth, despite using a double-blind condition for image segmentation and analysis, manual layer-by-layer delineation of the tumor ROI still relies on the subjective judgment of the radiologists. There may be variability in the delineation between different radiologists, especially when defining tumor boundaries or regions, which could be influenced by their experience and technical expertise. The use of deep learning algorithms, such as convolutional neural networks (CNNs), for automatic segmentation, combined with radiologists' review and correction, could reduce the error in manual segmentation, improving the consistency and efficiency of the delineation process.

Conclusion

Based on the results of this study, quantitative and semi-quantitative parameters from dynamic contrast-enhanced imaging (DCE-MRI) combined with diffusion kurtosis imaging (DKI) and intravoxel incoherent motion imaging (IVIM) full-field histogram parameters have significant clinical value in predicting the efficacy of neoadjuvant chemotherapy (NAC) in patients with invasive ductal carcinoma of the breast. Parameters such as Kep from DCE-MRI, MD from DKI, and D and f values from IVIM show significant differences between the NAC effective and non-effective groups, with strong correlations to the treatment outcome.In particular, the combined use of DCE-MRI, DKI, and IVIM histogram parameters significantly improves prediction accuracy, with high diagnostic efficacy reflected in the AUC, sensitivity, and specificity values.

Additionally, immunohistochemical markers (such as ER, PR, HER2 status) and tumor morphological features (such as margin morphology and internal enhancement patterns) also play important roles in determining NAC efficacy. The combination of these clinical features with imaging parameters further enhances the accuracy of efficacy prediction.This study provides clinicians with a

comprehensive predictive model based on imaging and immunohistochemical data, offering a more precise basis for assessing NAC efficacy in patients with invasive ductal carcinoma of the breast before and after treatment. It also supports individualized treatment decision-making.

Therefore, the combined application of DCE-MRI, DKI, and IVIM can serve as a powerful imaging tool for the early assessment and prediction of NAC efficacy in breast cancer patients, with broad clinical application prospects.

Author contributions

Xianglong Chen, and Yong Luo contributed equally to this work as first authors, Xianglong Chen, and Luo Yong developed the concept and discussed experiments and collaboratively drafting the initial version of the manuscript. Zhiming Xie and Yun Wen collected patient samples and data. Fangsheng Mou and Wenbing Zeng served as co-corresponding authors, providing overall guidance and supervision for the organization and development of the manuscript. All authors participated in the critical review, revision, and approval of the final version of the manuscript.

Funding

This study was supported by Chongqing Regional Key Disciplines (zdxk202116).

Data availability

The data supporting the findings of this study are available from the corresponding author upon reasonable request. All relevant data are included in the article. Due to privacy or ethical restrictions, certain data may not be publicly available.

Declarations

Ethics approval and consent to participate

The studies involving humans were approved by Ethics Committee of Chongqing University Three Gorges Hospital. The studies were conducted in accordance with the local legislation and institutional requirements (MR-50-23-026780). This study is a retrospective analysis and has received an exemption from the informed consent requirement.

Consent for publication

All data have been anonymized to adhere to ethical standards, with explicit consent obtained from the participants, and all authors have provided their consent for this manuscript's publication.

Competing interests

The authors declare no competing interests.

Author details

[1]School of Medical Imaging, North Sichuan Medical Univesity, Nanchong, Sichuan Province, China
[2]Department of Radiology, Three Gorges Hospital Affiliated to Chongqing University, Chongqing, China
[3]School of Medicine, Chongqing University, Chongqing, China

Received: 29 October 2024 / Accepted: 11 March 2025
Published online: 14 April 2025

References

1. Sung H, Ferlay J, Siegel RL, et al. Global cancer statistics 2020: GLOBOCAN estimates of incidence and mortality worldwide for 36 cancers in 185 countries. Cancer J Clin. 2021;71(3):209–49. https://doi.org/10.3322/caac.21660
2. Maccoll CE, Guillaume Paré, Salehi A, et al. Postneoadjuvant pure and predominantly pure intralymphatic breast carcinoma: case series and literature review. Am J Surg Pathol. 2020. https://doi.org/10.1097/PAS.0000000000001610
3. Hussein H, Abbas E, Keshavarzi S, et al. Supplemental breast cancer screening in women with dense breasts and negative mammography: a systematic review and meta-analysis[J/OL]. Radiology. 2023;306(3). https://doi.org/10.1148/radiol.221785
4. Zhang Y, Li M, Wang J, et al. Role of dynamic contrast-enhanced magnetic resonance imaging in assessing breast cancer: evaluation of the morphological characteristics and biological behavior. Eur J Radiol. 2019;114:38–45. https://doi.org/10.1016/j.ejrad.2019.03.010
5. Cai J, Zhang L, Yu L. Clinical applications of diffusion kurtosis imaging in oncology. Am J Roentgenol. 2020;215(1):46–55. https://doi.org/10.2214/AJR.20.23211
6. Comparison of the pre-treatment functional MRI metrics' efficacy in predicting locoregionally advanced nasopharyngeal carcinoma response to induction chemotherapy. Cancer Imaging. 2021;21(1):1–12.https://doi.org/10.1186/s40644-021-00428-0
7. Fusco R, Sansone M. Granata V, et al. Diffusion and perfusion MR parameters to assess preoperative short-course radiotherapy response in locally advanced rectal cancer: a comparative explorative study among standardized index of shape by DCE-MRI, intravoxel incoherent motion- and diffusion kurtosis imaging-derived parameters. Abdom Radiol. 2019;44(11):3683–700. https://doi.org/10.1007/s00261-018-1801-z
8. Granata V, Fusco R, Sansone M, et al. Magnetic resonance imaging in the assessment of pancreatic cancer with quantitative parameter extraction by means of dynamic contrast-enhanced magnetic resonance imaging, diffusion kurtosis imaging and intravoxel incoherent motion diffusion-weighted imaging. Therapeutic Adv Gastroenterol. 2019;175628481988505. https://doi.org/10.1177/1756284819885052
9. Li H, Zhao S, Hai F. The effect of histogram analysis of DCE-MRI parameters on differentiating renal tumors. Clin Lab. 2023;69(11). https://doi.org/10.7754/Clin.Lab.2023.221126
10. Li Q, Xiao Q, Yang M, et al. Histogram analysis of quantitative parameters from synthetic MRI: correlations with prognostic factors and molecular subtypes in invasive ductal breast cancer. Eur J Radiol. 2021;(3):109697. https://doi.org/10.1016/j.ejrad.2021.109697
11. Smith R, Williams P. Role of imaging in evaluating neoadjuvant chemotherapy response in breast cancer. Med Imaging Diagnosis. 2018;7(4):58–65. https://doi.org/10.1007/s12035-018-1413-6
12. Zhao D, Fu X, Rohr J, et al. Poor histologic tumor response after adjuvant therapy in basal-like HER2-positive breast carcinoma[J]. Pathol Res Pract. 2021;228:153677. https://doi.org/10.1016/j.prp.2021.153677
13. Huang Y, Le J, Miao A, et al. Prediction of treatment responses to neoadjuvant chemotherapy in breast cancer using contrast-enhanced ultrasound. AME publishing company. 2021;(4). https://doi.org/10.21037/GS-20-836
14. Li J, et al. Clinical response and pathological assessment in breast cancer after neoadjuvant chemotherapy: a retrospective study of 3,000 patients. Cancer Med. 2023;12(4):1242–52.
15. Wang L, et al. Pathological response to neoadjuvant chemotherapy in HER2-positive breast cancer and its impact on prognosis. Front Oncol. 2022;12:799346.
16. Galati F, Rizzo V, Moffa G, et al. Radiologic-pathologic correlation in breast cancer: do MRI biomarkers correlate with pathologic features and molecular subtypes?[J]. Eur Radiol Experimental. 2022;6(1):1–13. https://doi.org/10.1186/s41747-022-00289-7
17. Zhang L, Wang X, Li Y, et al. Evaluation of tumor shrinkage patterns and clinical-pathological factors associated with neoadjuvant chemotherapy in breast cancer. Breast Cancer Res Treat. 2021;189(2):249–59. https://doi.org/10.1007/s10549-021-06116-0
18. Ramtohul T, Tescher C, Vaflard P, et al. Prospective evaluation of ultrafast breast MRI for predicting pathologic response afterneoadjuvant therapies. Radiology. 2022;305(3):565–74. https://doi.org/10.1148/radiol.220389
19. Dou H, Li F, Wang Y, et al. Estrogen receptor-negative/progesterone receptor-positive breast cancer has distinct characteristics and pathologic complete response rate after neoadjuvant chemotherapy. Diagn Pathol. 2024;19(1). https://doi.org/10.1186/s13000-023-01433-6
20. Leon-Ferre RA, Hieken TJ, Boughey JC. The landmark series: neoadjuvant chemotherapy for triple-negative and HER2-positive breast Cancer. Ann Surg Oncol. 2021;28(4):2111–9. https://doi.org/10.1245/s10434-020-09480-9
21. Teruya N, Inoue H, Horii R, et al. Intratumoral heterogeneity, treatment response, and survival outcome of ER-positive HER2-positive breast cancer. Cancer Med. 2023;12(9):10526–35. https://doi.org/10.1002/cam4.5788

22. Peng JH, Zhang X, Song JL, et al. Neoadjuvant chemotherapy reduces the expression rates of ER, PR, HER2, Ki67, and P53 of invasive ductal carcinoma. Medicine. 2019;98(2). https://doi.org/10.1097/MD.0000000000013554
23. Zhang H, Wang Z, Liu W, et al. Breast-conserving surgery in triple-negative breast cancer: a retrospective cohort Study. Evid Based Complement Alternat Med. 2023;2023:1–8. https://doi.org/10.1155/2023/5431563
24. Chen W, Li FX, Lu DL, et al. Differences between the efficacy of HER2(2+)/FISH-positive and HER2(3+) in breast cancer during dual-target neoadjuvant therapy. Breast. 2023;71:69–73. https://doi.org/10.1016/j.breast.2023.07.008
25. Liang X, Chen X, Yang Z, et al. Early prediction of pathological complete response to neoadjuvant chemotherapy combining DCE-MRI and apparent diffusion coefficient values in breast cancer. BMC Cancer. 2022;22(1):1250. https://doi.org/10.1186/s12885-022-10315-x
26. Guo W, Zhang Y, Luo D, et al. Dynamic contrast-enhanced magnetic resonance imaging (DCE-MRI) for pretreatment prediction of neoadjuvant chemotherapy response in locally advanced hypopharyngeal cancer. Br J Radiol. 2020;93(1115):20200751. https://doi.org/10.1259/bjr.20200751
27. Zhang D, Geng X, Suo S, et al. The predictive value of DKI in breast cancer: does tumour subtype affect pathological response evaluations? Magn Reson Imaging. 2021;85:28–34. https://doi.org/10.1016/j.mri.2021.10.013
28. Liu W, Wei C, Bai J, et al. Histogram analysis of diffusion kurtosis imaging in the differentiation of malignant from benign breast lesions. Eur J Radiol. 2019;117:156–63. https://doi.org/10.1016/j.ejrad.2019.06.008
29. Histogram analysis in predicting the grade and histological subtype of meningiomas based on diffusion kurtosis imaging. Acta Radiol. 2020;61(9):1228–39. https://doi.org/10.1177/0284185119898656
30. Zheng D, Lai G, Chen Y, et al. Integrating dynamic contrast-enhanced magnetic resonance imaging and diffusion kurtosis imaging for neoadjuvant chemotherapy assessment of nasopharyngeal carcinoma. J Magn Reson Imaging. 2018. https://doi.org/10.1002/jmri.26164
31. Ai Z, Han Q, Huang Z, et al. The value of multiparametric histogram features based on intravoxel incoherent motion diffusion-weighted imaging (IVIM-DWI) for the differential diagnosis of liver lesions. Ann Transl Med. 2020;(18). https://doi.org/10.21037/ATM-20-5109
32. Kim Y, Kim SH, Lee HW, et al. Intravoxel incoherent motion diffusion-weighted MRI for predicting response to neoadjuvant chemotherapy in breast cancer. Magn Reson Imaging. 2018;48:27–33. https://doi.org/10.1016/j.mri.2017.12.018
33. Gao Y, Wu W, Zhang X, et al. The role of diffusion-weighted imaging and dynamic contrast-enhanced magnetic resonance imaging in the prediction of chemotherapy response in breast cancer. Eur J Radiol. 2019;116:159–65. https://doi.org/10.1016/j.ejrad.2019.04.022

Publisher's note